

Kolmogorov and Iroshnikov-Kraichnan scaling in the anisotropic turbulent solar wind.

Sandra C. Chapman* and Bogdan Hnat

*Centre for Fusion, Space and Astrophysics, Physics Department,
University of Warwick, Coventry, CV4 7AL, UK.*

(Dated: September 6, 2018)

Solar wind turbulence is dominated by Alfvénic fluctuations but the power spectral exponents somewhat surprisingly evolve toward the Kolmogorov value of $-5/3$, that of hydrodynamic turbulence. We show that at 1AU the turbulence decomposes linearly into two coexistent components perpendicular and parallel to the local average magnetic field. The first of these is consistent with propagating Alfvén wavepackets and shows the scaling expected of Alfvénic turbulence, namely Iroshnikov-Kraichnan. The second shows Kolmogorov scaling which we also find in the number and magnetic energy density, and Poynting flux.

PACS numbers: 96.50.Ci, 52.30.Cv, 52.35.Ra, 95.30.Qd

The solar wind provides a unique laboratory for the study of Magnetohydrodynamic (MHD) turbulence with a magnetic Reynolds number estimated to exceed 10^5 in the solar wind[1]. In-situ satellite observations of bulk plasma parameters strongly suggest the presence of turbulence via the statistical properties of their fluctuations[2, 3]. Quantifying these fluctuations is also central to understanding both the transport of solar energetic particles and galactic cosmic rays within the heliosphere, and solar wind evolution with implications for the mechanisms that accelerate the wind at the corona.

The observed fluctuations in the solar wind present a complex mixture of hydrodynamic and Alfvénic signatures. Alfvénic fluctuations dominate the power in these fluctuations and are observed propagating away from the sun implying solar origin (e.g. [4]). However the power spectra [2, 3, 4, 5] suggest an exponent evolving toward the Kolmogorov[6] (hereafter K-41) value of $\sim 5/3$, that of hydrodynamic turbulence. This is paradoxical since for ideal MHD the turbulent cascade is expected to be mediated via Alfvén wavepackets suggesting an exponent of $\sim -2/3$, that of Iroshnikov and Kraichnan[7] (hereafter IK). Intervals can be found where different magnetic field and velocity components simultaneously exhibit K-41 and IK scaling[8, 9], indeed, these phenomenologies can be difficult to distinguish in low order moments[10]. The flow is also observed to be intermittent, this has been suggested to account for the 'anomalous' $-5/3$ scaling in the power spectra in terms of incompressible MHD, rather than hydrodynamic, phenomenology[11]. Alfvénic fluctuations, when isolated by the use of Elsasser variables (see e.g.[4]), and decomposed by considering different average magnetic field orientations that occur at different times, are found to be multicomponent[12], and coupled[13]. This picture, of an essentially incompressible, multicomponent Alfvénic turbulence[4, 12] suggests that a significant population of Alfvénic fluctuations evolve to have wavevectors almost perpendicular to the

background magnetic field, leading to a 'fluid-like' (in the sense of K-41) phenomenology, and the $-5/3$ power spectral slope. However, fluctuations in solar wind density are not simply proportional to that in magnetic field[14] and show nontrivial scaling[2, 15] that suggests that the turbulence is compressible[16]. The role of compressibility is thus an open question. An important corollary is that the full behaviour cannot be captured by models which describe the observed Alfvénic properties in terms of fluctuating coronal fields that have advected passively in the expanding solar wind[17].

Here, we will quantify the interplay between K-41 and IK phenomenologies in the turbulent solar wind. We can discuss the statistical properties of fluctuations in some variable of the flow, such as velocity, magnetic field, or density, by considering ensemble averages. Fluctuations in the velocity field can be characterized by the difference in some component, or in the magnitude, $\delta v = v(r+L) - v(r)$ at two points separated by distance L . The dependence of δv upon L is determined in a statistical sense through the moments $\langle \delta v^p \rangle$, where $\langle \dots \rangle$ denotes an ensemble average over r . Statistical theories of turbulence then anticipate scaling $\langle \delta v_L^p \rangle \sim L^{\zeta(p)}$.

Kolmogorov's 1941 theory for hydrodynamic flows[6] essentially follows from dimensional analysis. A fluctuation δv arising from a transient structure in the flow with characteristic lengthscale L , and timescale T , transfers kinetic energy δv^2 implying an energy transfer rate $\epsilon_L \sim \delta v^2/T \sim \delta v^3/L$. If the statistics of the fluctuations in the energy transfer rate are independent of L , its p moments $\langle \epsilon_L^p \rangle \sim \epsilon_0^p$ where the constant ϵ_0 is the average rate of energy transfer. This gives the K-41 scaling $\langle \delta v_L^p \rangle \sim L^{p/3}$. In practice, hydrodynamic flows are found to deviate from this simple scaling. This intermittency[18] is introduced through a lengthscale dependence of the fluctuations in energy transfer rate so that $\langle \epsilon_L^p \rangle \sim \epsilon_0^p (L/L_0)^{\mu(p)}$, where L_0 is some characteristic lengthscale and $\mu(p)$ is the intermittency correction. The scaling for the moments then becomes $\langle \delta v_L^p \rangle \sim L^{\zeta(p)}$ with the K-41 exponents $\zeta(p) = p/3 - \mu(p/3)$. For incompressible MHD turbulence, Alfvénic phenomenology mediates the cascade, introducing an additional char-

*Electronic address: S.C.Chapman@warwick.ac.uk

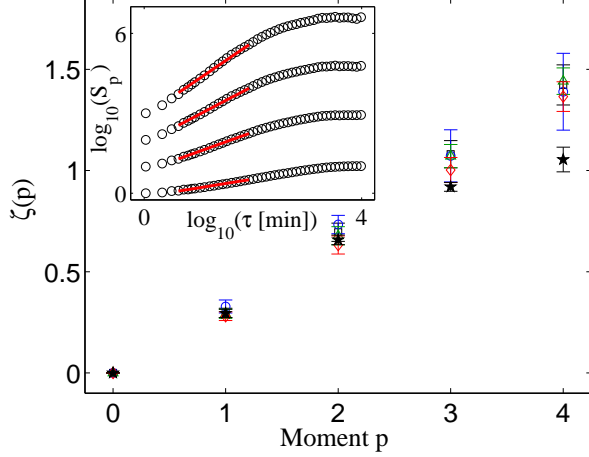


FIG. 1: Structure function analysis of solar wind density fluctuations. Inset: structure functions versus differencing interval τ (the traces are offset for clarity). Main plot: scaling exponents computed from the raw data (\star), and applying an upper limit to fluctuation size of $20\sigma(\tau)$ (\square), $15\sigma(\tau)$ (\circ), $10\sigma(\tau)$ (\triangle) and $5\sigma(\tau)$ (\diamond).

acteristic speed, the Alfvén speed v_A . The above dimensional argument then gives an energy transfer rate $\epsilon_L \sim (\delta v^2/T)(\delta v/v_A) \sim \delta v^4/L$, which is just that proposed by Iroshnikov and Kraichnan[7], so that $\langle \delta v^p \rangle \sim L^{\zeta(p)}$ now with $\zeta(p) = p/4 - \mu(p/4)$.

The experimental study of turbulence then centres around measurement of the scaling exponents, the $\zeta(p)$. A full description requires the (difficult to determine) intermittency correction, the $\mu(p)$. However, if the system is in a homogeneous steady state, the average energy transfer rate is uniform so that $\langle \epsilon_L \rangle = \epsilon_0$ and $\mu(1) = 0$ giving, for K-41 $\zeta(3) = 1$, and for IK, $\zeta(4) = 1$, independent of the intermittency of the flow. A determination of the lower order moments that is sufficiently accurate to distinguish these two cases is possible for in-situ observations of the solar wind and we present this here. These observations are typically time series from a single spacecraft so that the ensemble averages that we will consider will be over time rather than over space, the spatial separation L above being replaced by a time interval τ - the Taylor hypothesis[1]. Consistent with almost all experimental studies of turbulence we consider generalized structure functions of a given parameter x : $S_p(\tau) = \langle |x(t+\tau) - x(t)|^p \rangle$. Solar wind monitors such as the ACE spacecraft spend several-year long periods in orbit about the Lagrange point sunward of the earth. We analyse 64s averaged plasma parameters from ACE for the interval 01/01/1998 - 12/31/2001, this consists of $\sim 1.6 \times 10^6$ samples and is dominated by slow solar wind. Figure 1 shows the procedure for extracting the scaling exponents from the data. The inset panel shows the structure functions of fluctuations in the density versus differencing interval for $p = 1-4$. There is a scaling range for timescales of minutes up to a few hours, the timescale

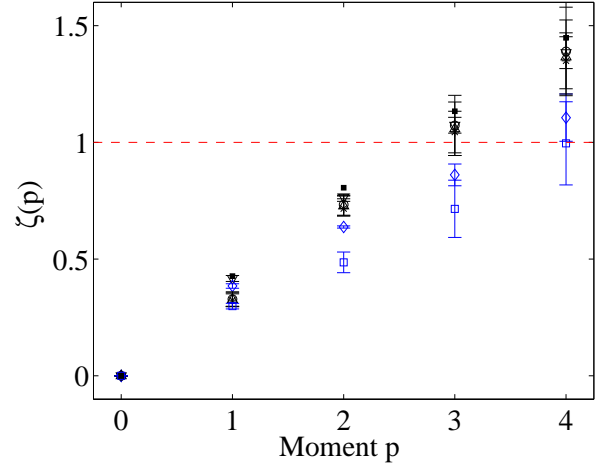


FIG. 2: Scaling exponents $\zeta(p)$ versus p for solar wind quantities, in blue, magnitudes of velocity v (\square) and magnetic field B (\diamond), in black, number density ρ (\circ), number flux ρv (\triangle) and momentum flux ρv^2 (\diamond), magnetic energy density B^2 (∇) and Poynting flux vB^2 (\blacksquare). Note that $\zeta(4) \approx 1$ and $\zeta(3) \approx 1$ respectively for these groups of quantities.

for large scale coherent structures. This scaling range has been shown to extend up to almost three orders of magnitude via Extended Self Similarity (ESS)[16]. The scaling exponents, that is, the $\zeta(p)$, where $S_p(\tau) \sim \tau^{\zeta(p)}$, are the gradients of these scaling regions, and these are shown in the main plot. The error bars provide an estimate of the uncertainty in the gradients of the fitted lines (linear regression error). Finite, experimental data sets include a small number of extreme events which have poor representation statistically and may obscure the scaling properties of the time series. One method[8, 19] for excluding these rare events is to fix a (large) upper limit on the magnitude of fluctuations used in computing the structure functions. Importantly, this limit is varied with the temporal scale τ to account for the growth of range with τ in the time series. The figure shows the exponents computed for a range of values for this upper limit $[5, 20]\sigma(\tau)$, where $\sigma(\tau) = S_2^{1/2}$. We see that the scaling exponents are insensitive to the value of the upper limit once a limit is applied and the rare large events are removed. Above $10\sigma(\tau)$ this process eliminates less than 1% of the data points.

We now compare the scaling exponents for different scalar quantities in the solar wind flow, for structure functions up to $p = 4$. In Figure 2 we show the scaling exponents for fluctuations in the magnitude of velocity v and magnetic field B (blue symbols), along with those for the number density ρ , the magnetic energy density B^2 , the flux density ρv^2 and the Poynting flux in the MHD limit vB^2 (black symbols). The scaling exponents for these low order structure functions are determined with sufficient precision that we can see that in the case of the velocity and magnetic field magnitudes, the $\zeta(4)$ ex-

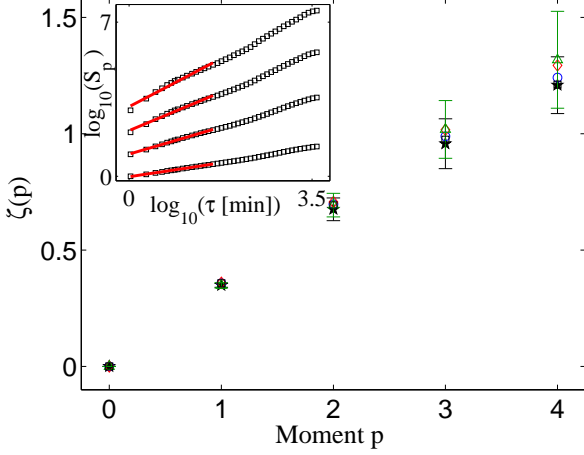


FIG. 3: Structure function analysis of $\langle |\delta \mathbf{v} \cdot \hat{\mathbf{b}}|^p \rangle$. Inset: structure functions versus differencing interval (the traces are offset for clarity). Main plot: scaling exponents computed from the raw data (\star), and applying an upper limit to fluctuation size of $20\sigma(\tau)$ (\square), $15\sigma(\tau)$ (\circ), $10\sigma(\tau)$ (\triangle) and $5\sigma(\tau)$ (\diamond).

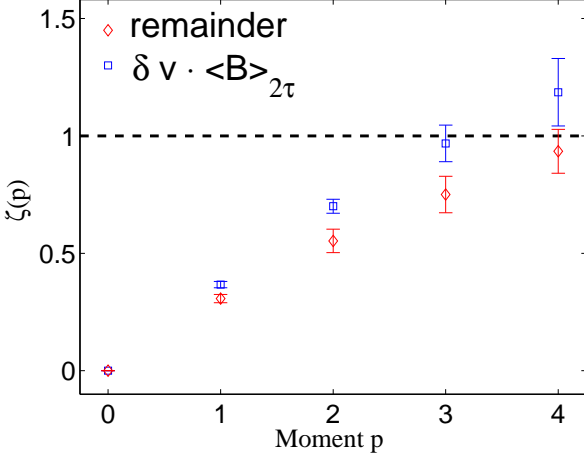


FIG. 4: Scaling exponents $\zeta(p)$ versus p for the structure functions of $\langle |\delta \mathbf{v} \cdot \hat{\mathbf{b}}|^p \rangle$ (\square) and of the remaining signal (\diamond). Note that $\zeta(3) \approx 1$ and $\zeta(4) \approx 1$ respectively for these quantities.

ponents are clustered about unity, whereas for the other quantities, the $\zeta(3)$ exponents are clustered about unity. Thus the fluctuations in velocity and magnetic field magnitude appear to be dominated by Alfvénic processes, in the sense of IK phenomenology, whereas the fluctuations in the magnetic field energy, plasma and flux densities are hydrodynamic-like, in the sense of K-41. Intriguingly, these two phenomenologies are coexistent.

We now introduce an operation that 'filters out' one of the relevant physical processes, namely, Alfvénic fluctuations. We exploit the property that the full non-linear MHD equations support large scale Alfvénic fluctua-

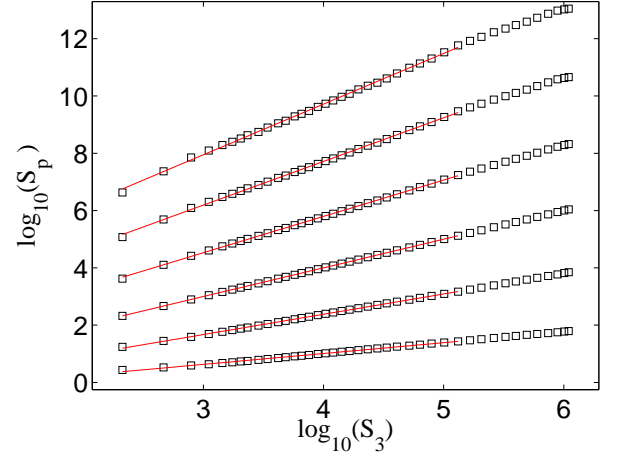


FIG. 5: Structure functions S_p versus S_3 for $p = 1 - 6$ for $S_p = \langle |\delta \mathbf{v} \cdot \hat{\mathbf{b}}|^p \rangle$. The traces are offset for clarity.

tions which share a basic property of Alfvén waves- that the velocity perturbation is perpendicular to the background magnetic field. In the turbulent flow, the magnetic field also fluctuates, but we can consider a local background value by constructing a running average of the vector magnetic field over the timescale τ' . For each interval over which we obtain a *difference* in velocity $\delta \mathbf{v} = \mathbf{v}(\mathbf{t} + \tau) - \mathbf{v}(\mathbf{t})$ we also obtain a vector *average* for the magnetic field direction $\hat{\mathbf{b}} = \bar{\mathbf{B}} / |\bar{\mathbf{B}}|$ from a vector sum of all the observed vector values between t and $t + \tau'$, $\bar{\mathbf{B}}(\mathbf{t}, \tau') = \mathbf{B}(\mathbf{t}) + \dots + \mathbf{B}(\mathbf{t} + \tau')$, with τ' centred on τ . We choose the interval $\tau' = 2\tau$ here as the minimum (Nyquist) necessary to capture wavelike fluctuations. Velocity differences $\delta \mathbf{v}$ which are Alfvénic in character will then have the property that the scalar product $\delta \mathbf{v} \cdot \hat{\mathbf{b}}$ will vanish. This condition filters out *all* those fluctuations which generate a velocity displacement perpendicular to the local magnetic field, and is thus less restrictive than the Elsasser[4] variables which select propagating pure Alfvén waves. In Figure 3 we plot the structure functions of the quantity $\delta v_{\parallel} = \delta \mathbf{v} \cdot \hat{\mathbf{b}}$, that is, $S_p = \langle |\delta \mathbf{v} \cdot \hat{\mathbf{b}}|^p \rangle$ versus τ , (inset) and the corresponding scaling exponents, the $\zeta(p)$ for the region where $S_p \sim \tau^{\zeta(p)}$ (main plot) generated in the same way as in Figure 1. In Figure 4 we compare these exponents with those obtained for the remaining signal, that is, $\delta v_{\perp} = \sqrt{(\delta \mathbf{v} \cdot \delta \mathbf{v} - (\delta \mathbf{v} \cdot \hat{\mathbf{b}})^2)}$. Remarkably, both these quantities show a clear scaling range (which we will verify) with scaling exponents $\zeta(3)$ and $\zeta(4)$ close to unity for δv_{\parallel} and δv_{\perp} respectively.

This result is consistent with the fluctuations in velocity being a simple linear superposition that are close to (i) parallel to the local background magnetic field and sharing hydrodynamic-like scaling, that is K-41, with that of the number, magnetic energy and flux densities, and (ii) perpendicular to the local background magnetic field with the scaling expected of Alfvénic turbulence in the sense of IK. These results provide the first unam-

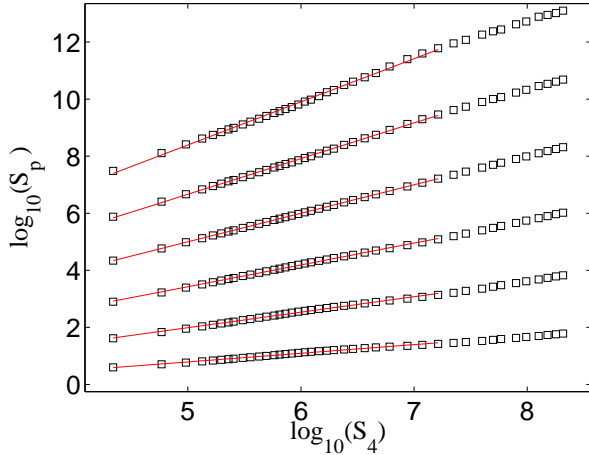


FIG. 6: Structure functions S_p versus S_4 for $p = 1 - 6$ for $S_p = \langle |\sqrt{\delta \mathbf{v} \cdot \delta \mathbf{v} - (\delta \mathbf{v} \cdot \hat{\mathbf{b}})^2}|^p \rangle$. The traces are offset for clarity.

biguous ordering of the data with respect to hydrodynamic (i.e. Kolmogorov-like), and Alfvénic (i.e. Iroshnikov-Kraichnan-like) phenomenology in different parameters observed at a single location in the solar wind.

We verify that these quantities indeed show an extended scaling region by means of ESS[20]. If the scaling is such that the $S_p \sim S_q^{\zeta(p)/\zeta(q)}$ then a plot of S_p versus S_q will reveal the range of the underlying power law dependence with τ . If, as here, one of the $\zeta(p)$ are close to unity, the ESS plot will in addition provide a better estimate of the $\zeta(p)$. Figures 5 and 6 show S_p versus S_3 for δv_{\parallel} and versus S_4 for δv_{\perp} respectively, and we see that there is scaling over several orders of magnitude.

The slopes of these plots imply exponents that are multifractal, that is, quadratic in p , and distinct for the two cases.

The characteristic nature of solar wind turbulence is revealed to be a coexistence of two signatures. The first of these is consistent with Alfvénic turbulence in the sense of IK mediated by Alfvén wavepackets propagating parallel to the magnetic field. The second, which shows K-41 scaling, has a compressive component and could couple nonlinearly into strongly oblique, almost non propagating Alfvénic fluctuations. This clearly elucidates the previously proposed multicomponent nature of solar wind turbulence and suggests one of two scenarios. The first of these is that the turbulent solar wind is comprised of two weakly interacting components- one from the process that generates the solar wind at the corona and the other that evolves in the high Reynolds number flow. Given the evidence for outward propagating Alfvén waves and evolution toward K-41 scaling, these correspond to IK, and K-41 phenomenology respectively and our result yields an important insight into the physics of solar wind generation. Alternatively, the coexistence of the two components is characteristic of the anisotropic nature of compressible MHD turbulence in the presence of a background field, in which case this determination of their scaling properties points to an important modification of theories of MHD turbulence.

I. ACKNOWLEDGMENT

The authors thank G. Rowlands for discussions, the ACE Science Centre for data provision and the PPARC for support.

-
- [1] W. H. Matthaeus, S. Dasso, J. M. Weygand, L. J. Milano, C. W. Smith, M. G. Kivelson, Phys. Rev. Lett., **95**, 231101, (2005)
 - [2] C.-Y. Tu and E. Marsch, Space Sci. Rev. **73**, 1, (1995).
 - [3] M. L. Goldstein, Astrophys. Space Sci., **277**, 349, (2001)
 - [4] T.S.Horbury, M. A. Forman, S. Oughton, Plasma Phys. Cont. Fusion, **47**, B703, (2005)
 - [5] S. D. Bale, P. J. Kellogg, F. S. Mozer, T. S. Horbury, H. Reme, Phys. Rev. Lett., **94**, 215002, (2005)
 - [6] A. N. Kolmogorov, C. R. Acad. Sci., **30**, 301, (1941)
 - [7] P. S. Iroshnikov, Sov. Astron., **7**, 566, (1964); R. H. Kraichnan, Phys. Fluids, **8**, 1385, (1965)
 - [8] P. Veltri, Plasma Phys. Cont. Fusion, **41**, A787, (1999)
 - [9] A. Bershadskii, Phys. Rev. E, **66**, 046410, (2002)
 - [10] V. Carbone, P. Veltri, R. Bruno, Phys. Rev. Lett., **75**, 3110, (1995)
 - [11] V. Carbone, Phys. Rev. Lett., **71**, 1546, (1993)
 - [12] W. H. Matthaeus, M. L. Goldstein, D. A. Roberts, J. Geophys. Res., **87**, 10347, (1990)
 - [13] L. J. Milano, S. Dasso, W. H. Matthaeus, C. W. Smith, Phys. Rev. Lett., **93**, 155005, (2004)
 - [14] S. R. Spangler, L. G. Spiller, Phys. Plasmas, **11**, 1969, (2004)
 - [15] B. Hnat, S. C. Chapman and G. Rowlands, Phys. Rev. E **67**, 056404 (2003)
 - [16] B. Hnat, S. C. Chapman, G. Rowlands, Phys. Rev. Lett., **94**, 204502, (2005)
 - [17] J. Giacalone, J. R. Jokipii, W. H. Matthaeus, Ap. J., **641**, L61, (2006)
 - [18] U. Frisch, *Turbulence. The legacy of A.N. Kolmogorov* (Cambridge University Press, Cambridge, 1995).
 - [19] S. C. Chapman, B. Hnat, G. Rowlands, Nonlin. Proc. Geophys., **12**, 767, (2005)
 - [20] R. Benzi, S. Ciliberto, C. Baudeta and G. R. Chavarria, Physica D **80**, 385, (1995).